Optimizing the optical field distribution of solid immersion lens system by a continuous phase filter

Xuehua Ye (叶雪华), Yaoju Zhang (张耀举), and Junfeng Chen (陈俊峰)

College of Physics and Electronic Information, Wenzhou University, Wenzhou 325027

Received November 30, 2006

In solid immersion lens (SIL) microscopy systems with high numerical aperture (NA), there always exists the aberration produced by Fresnel effects at the interface between SIL and the sample. This aberration may cause the degradation of the image of sample. We design a continuous phase filter and optimize the optical field distribution of SIL system. The numerical results show that when the continuous phase filter is used, the field distribution of SIL system can be optimized, and the focal depth and intensity of transmitted light can be increased. At the same time, the intensity of side-lobe and the resolution are kept almost unchanged.

OCIS codes: 050.1970, 210.0210, 230.0230.

The technique of solid immersion lens (SIL), which can overcome the diffraction limit, was first proposed by Mansfield and Kino in 1990[1]. Since then, various applications of SILs have been developed, such as optical storage[2−4], scanning microscopy[5], photolithography[6], the study of semiconductor structures[7], and other applications[8−10]. Among them, two types of SILs are being widely developed, one is hemisphere SIL (h-SIL) and the other is super-hemisphere SIL (s-SIL). To further improve the resolution of SIL microscopy system, the two-zone amplitude filters[11,12] or phase filters[13,14] have been used for high numerical aperture (NA) SIL systems. However, these amplitude filters may result in reduction of focal depth or Strehl ratio, which is a drawback to their application. Although a discrete phase filter can increase the focal depth of a SIL system in some extent, the Strehl ratio still is not high enough and the side-lobe intensity is large. Recently, we proposed a three-zone amplitude filter and a phase filter[15,16]. Both of them can increase the focal depth and improve the resolution of SIL systems, but they still cannot avoid the energy loss. In the near-field microscopy, the improvement of lateral resolution is required, and the long focal depth and high Strehl ratio are useful to many applications such as optical storage and photolithography, especially in improving the collection efficiency of single-photon emitters[10]. However, the aberration at the interface between SIL and the sample may degrade the image of sample in the near field. In order to corrent the aberration of SIL system, Zhang has proposed a unique design of SIL system by changing the radius or thickness[17]. In this letter, we introduce a filter that has a continuously varying phase to eliminate influence of aberration. This filter can increase largely Strehl ratio and focal depth of the SIL systems, and keep the side-lobe intensity and resolution almost unchanged.

The schematic of the SIL system optimized by a continuous phase filter is illuminated in Fig. 1. The thickness of the SIL is $h = R + A$, where A is the distance from the plane surface to the center of the sphere and R is the radius of the SIL. Supposing the SIL is surrounded by air, the distance from Gaussian focus of the converging lens to the center of the SIL is L ($L + R < f_0$, f_0 is the focal length of the converging lens). The phase filter is placed closely in front of a converging lens L_1 with a high NA and the SIL is on the right side of L_1. The origin O on the plane surface of the SIL is at the focus of the system. Following the procedure of Helseth[18] and Török *et al.*[19], we obtain the transmitted field of a general SIL system near the focus,

$$\mathbf{E} = \int_0^{\theta_{2\max}} \mathrm{d}\theta \int_0^{2\pi} \mathbf{A}(\theta_1, \phi) \exp(ik_3 z_3 \cos\theta_3) \times \exp[ik_2 \rho_c \sin\theta_2 \cos(\phi - \phi_c)] \exp(ik_0 \psi_G) \sin\theta_2 \mathrm{d}\phi, \quad (1)$$

where $\theta_{2\max}$ is the maximum effective converging angle of light in the medium 2, k_i ($i = 1, 2, 3$) is the wave number in the medium i, k_0 is the wave number in vacuum, ψ_G is the geometric aberration function of the SIL, and (ρ_c, z_c, ϕ_c) are cylindrical coordinates centered at the plane surface of the SIL. The relationship between the maximum effective converging angle of the SIL and the maximum converging angle α of the lens is given by

$$\theta_{2\max} = \alpha + \arcsin\left(\frac{A}{R}\frac{n_2 \sin\theta_{2\max}}{n_1}\right) - \arcsin\left(\frac{A}{R}\sin\theta_{2\max}\right). \quad (2)$$

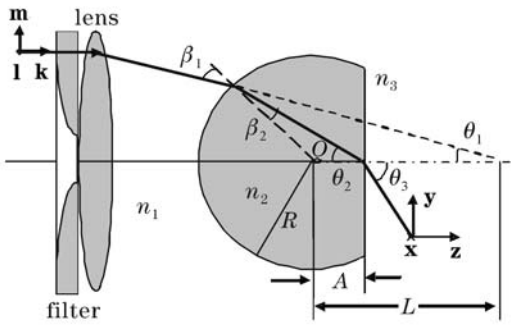

Fig. 1. Schematic of the SIL system.

$\mathbf{A}(\theta_1,\phi)$ in Eq. (1) is the vector pupil distribution,

$$\mathbf{A}(\theta_1,\phi)=\mathbf{P}(\theta_1,\phi)\sqrt{\cos\theta_1}, \tag{3}$$

where $\sqrt{\cos\theta_1}$ is the apodization function, $\mathbf{P}(\theta_1,\phi)$ is the polarization vector, which has been derived as

$$\mathbf{P}(\theta_1,\phi)=\begin{bmatrix} t_{1\mathrm{p}}t_{2\mathrm{p}}\cos\phi(a\cos\phi+b\sin\phi)\cos\Theta-t_{1\mathrm{s}}t_{2\mathrm{s}}\sin\phi(-a\sin\phi+b\cos\phi)\\ t_{1\mathrm{p}}t_{2\mathrm{p}}\sin\phi(a\cos\phi+b\sin\phi)\cos\Theta+t_{1\mathrm{s}}t_{2\mathrm{s}}\cos\phi(-a\sin\phi+b\cos\phi)\\ -t_{1\mathrm{p}}t_{2\mathrm{p}}(a\cos\phi+b\sin\phi)\sin\Theta\end{bmatrix}, \tag{4}$$

$$\begin{aligned}&\Theta=\theta_1+\beta_1+\theta_3-\beta_2-\theta_2,\\ &\beta_1=\arcsin(An_2\sin\theta_2/Rn_1),\\ &\beta_2=\arcsin(A\sin\theta_2/R),\\ &\theta_1=\theta_2-\beta_1+\beta_2,\\ &\theta_3=\arcsin(n_2\sin\theta_2/n_3),\end{aligned} \tag{5}$$

where $t_{1\mathrm{p}}$, $t_{1\mathrm{s}}$ and $t_{2\mathrm{p}}$, $t_{2\mathrm{s}}$ are the Fresnel transmission coefficients at the spherical and planar interfaces, respectively, a and b are the parameters describing an incident polarization $\mathbf{P}_0$,

$$\mathbf{P}_0=\begin{bmatrix} a(\theta_1,\phi)\\ b(\theta_1,\phi)\\ 0\end{bmatrix}. \tag{6}$$

Supposing that the radial polarized plane wave illuminates the system, Eq. (4) can be simplified as

$$\mathbf{P}(\theta_1,\phi)=\begin{bmatrix} t_{1\mathrm{p}}t_{2\mathrm{p}}\cos\phi\cos\Theta\\ t_{1\mathrm{p}}t_{2\mathrm{p}}\sin\phi\cos\Theta\\ -t_{1\mathrm{p}}t_{2\mathrm{p}}\sin\Theta\end{bmatrix}. \tag{7}$$

The geometric aberration function ψ_{G} is similar to that in Ref. [20],

$$\begin{aligned}\psi_{\mathrm{G}}=&R(1-n_2)+n_2A(\cos\theta_2-1)+L\\ &+n_2\sqrt{R^2-A^2\sin^2\theta_2}-(R^2+L^2\\ &+2L[-A\sin^2\theta_2+\cos\theta_2\sqrt{R^2-A^2\sin^2\theta_2}])^{1/2}.\end{aligned} \tag{8}$$

When $A=L=0$ for h-SIL and $A=R/n_2$, $L=n_2R$ (n_2 is the refractive index of the SIL) for s-SIL, the two SIL systems are aplanatic and consequently the geometric aberration ψ_{G} in Eq. (8) is equal to zero. Substituting Eqs. (3), (7), and (8) into Eq. (1) and performing the integral for the angle ϕ, we obtain

$$\begin{aligned}&E_x=iI_1\cos\phi_{\mathrm{c}},\\ &E_y=iI_1\sin\phi_{\mathrm{c}},\\ &E_z=-2I_0,\\ &I_1=\int_0^{\theta_{2\max}}t_{1\mathrm{p}}t_{2\mathrm{p}}T(\theta_2)\sqrt{\cos\theta_1}\sin\theta_2\cos\Theta\\ &\quad\times\exp(ik_3z_{\mathrm{c}}\cos\theta_3)J_1(k_2\rho_{\mathrm{c}}\sin\theta_2)\mathrm{d}\theta_2,\\ &I_0=\int_0^{\theta_{2\max}}t_{1\mathrm{p}}t_{2\mathrm{p}}T(\theta_2)\sqrt{\cos\theta_1}\sin\theta_2\cos\Theta\\ &\quad\times\exp(ik_3z_{\mathrm{c}}\cos\theta_3)J_0(k_2\rho_{\mathrm{c}}\sin\theta_2)\mathrm{d}\theta_2,\end{aligned} \tag{9}$$

where $T(\theta_2)$ is the effective transmittance function of the phase-only filter, J_n is the nth Bessel function of first kind. To describe the characteristic of rotating symmetry of light field, we transform the expression of electric field in Cartesian coordinates (Eq. (10)) into cylindrical coordinates and find that the azimuthal element is zero. The longitudinal and transverse elements can be determined by

$$\begin{aligned}E_\rho=&i\int_0^{\theta_{2\max}}t_{1\mathrm{p}}t_{2\mathrm{p}}T(\theta_2)\sqrt{\cos\theta_1}\sin\theta_2\cos\Theta\\ &\times\exp(ik_3z_{\mathrm{c}}\cos\theta_3)J_1(k_2\rho_{\mathrm{c}}\sin\theta_2)\mathrm{d}\theta_2,\\ E_z=&2\int_0^{\theta_{2\max}}t_{1\mathrm{p}}t_{2\mathrm{p}}T(\theta_2)\sqrt{\cos\theta_1}\sin\theta_2\sin\Theta\\ &\times\exp(ik_3z_{\mathrm{c}}\cos\theta_3)J_0(k_2\rho_{\mathrm{c}}\sin\theta_2)\mathrm{d}\theta_2.\end{aligned} \tag{11}$$

From Eq. (11) it is found that the optical field distribution of SIL system is related to the Fresnel transmission coefficient $t_{2\mathrm{p}}$, which is written as

$$\begin{aligned}&t_{2\mathrm{p}}=\frac{2n_2\cos\theta_2}{n_3\cos\theta_2+n_2\cos\theta_3},\\ &\theta_3=\arcsin(n_2\sin\theta_2/n_3).\end{aligned} \tag{12}$$

Figure 2 shows the phase transmittances. All plane-wave components with incident angles in the range of $\theta_2\in[0,\theta_{\mathrm{c}}]$, where θ_{c} is the critical angle of the total reflection, have real transmission coefficients. Consequently, there are no phase shifts between incident and transmitted waves at the interface. However, plane-wave components in the range of $\theta_2\in[\theta_{\mathrm{c}},\theta_{2\max}]$ undergo total reflection at the interface, and the transmission coefficients become complex. These complex transmission coefficients impose a phase shift between incident and transmitted waves that can be viewed as an additional aberration between the incident and transmitted waves, as shown in Fig. 2. The additional aberration can be described as

$$\psi_F=\begin{cases}\arctan(-n_2\sqrt{(n_2\sin\theta_2)^2-1}/\cos\theta_2), & \theta_2>\theta_{\mathrm{c}}\\ 0, & \theta_2\le\theta_{\mathrm{c}}\end{cases}. \tag{13}$$

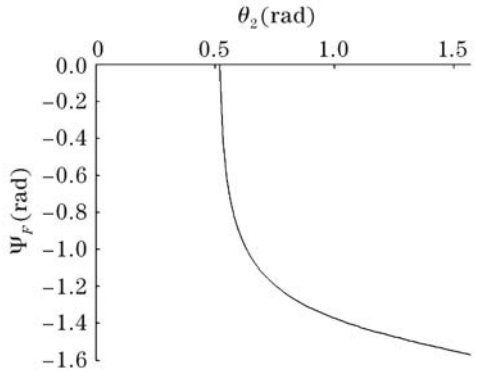

Fig. 2. Phase transmittance according to the Fresnel transmission coefficient.

This aberration may cause degeneration of image quality in optical field distribution of SIL system. In order to overcome the influences of the aberration completely, the transmittance function of the designed phase filter is

$$T(\theta_2) = \begin{cases} 1, & 0 \le \theta_2 \le \theta_c \\ \mathrm{e}^{-i\psi_F}, & \theta_c \le \theta_2 \le \theta_{2\max} \end{cases} . \quad (14)$$

Now let us analyze the effects of an inserted continuous phase filter on the transmitted fields of h- and s-SIL systems, respectively. At the same time, we compare the effects of designed phase filter with the annular amplitude filter proposed by Lu *et al.*[11], which is with the transmittance function of

$$T(\theta_2) = \begin{cases} 0, & 0 \le \theta_2 \le \theta_c \\ 1^F, & \theta_c \le \theta_2 \le \theta_{2\max} \end{cases} . \quad (15)$$

Both the h- and s-SILs are with the refractive index of $n_2 = 2$, and the illuminating wavelength of diode laser is 0.65 μm. For the h-SIL system, the NA of converging lens is chosen as 0.707, therefore the effective NA of h-SIL system is $\mathrm{NA_e} = 1.414$. For s-SIL system, NA =0.433 and $\mathrm{NA_e} = 1.732$.

The transverse and axial intensity distributions of the s-SIL system in focal region are shown in Figs. 3(a) and (b), respectively. Figure 4 shows the case for the h-SIL system. For comparison, we also plot the intensity distributions with the annular amplitude filter.

By comparing the cases with and without the continuous phase filter, it is found that the designed phase filter can increase the intensity of focal spot and the focal depth defined as the axial full-width at half-maximum (FWHM). In the s-SIL system, the continuous phase filter increases the intensity of focal spot and the focal depth by 30% and 25.1%, respectively. At the same time, the maximal side-lobe intensity is reduced from 8.1% to 6.3% and the focal spot size keeps almost unchanged. However, the annular amplitude filter decreases both the intensity of the focal spot and the focal depth. In the h-SIL system, the increases in the intensity of focal spot and the focal depth are 27.6% and 30%, respectively, when the continuous phase filter is added. The side-lobe intensity is suppressed well while the focal spot size is almost constant. Reversely, the intensity of the focal spot and the focal depth are decreased greatly when using the annular amplitude filters. At the same time, by comparing Fig. 3 and Fig. 4, it is found that s-SIL can achieve smaller focal spot size and stronger intensity of focal spot than h-SIL. However, h-SIL can produce longer focal depth than s-SIL.

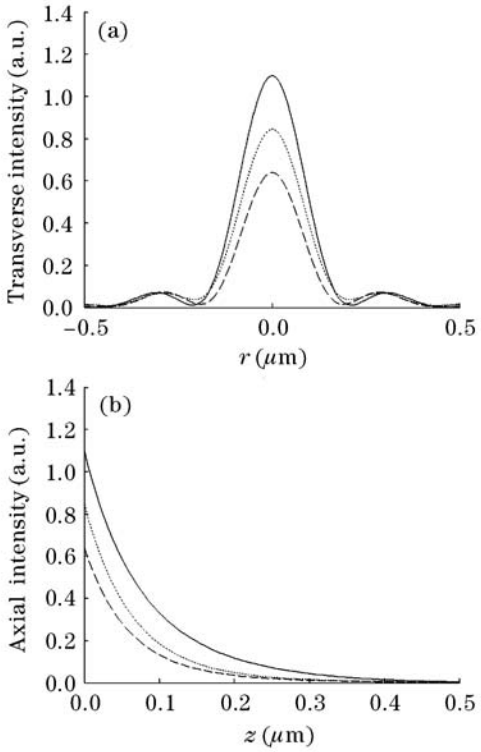

Fig. 3. (a) Transverse and (b) axial intensity distributions of the s-SIL system. The solid, dotted, and dashed curves are the cases with phase filter, without filter, and with amplitude filter, respectively.

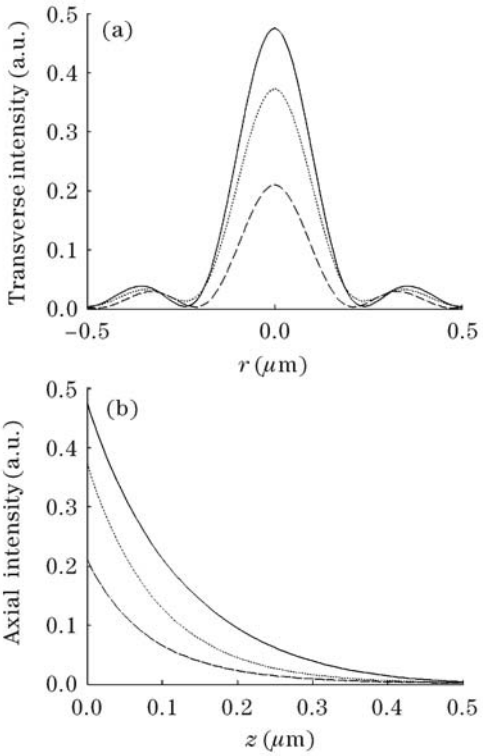

Fig. 4. (a) Transverse and (b) normalized axial intensity distributions of the h-SIL system. The solid, dotted, and dashed curves are the cases with phase filter, without filter, and with amplitude filter, respectively.

A physical model of the continuously varying phase filter is proposed and the optical field distribution of SIL system is optimized. The effects of the continuous phase filter are compared with that of an annular amplitude filter[11]. The numerical results show that the continuous phase filter increases the intensity of focal spot and the focal depth markedly for both h- and s-SIL systems. At the same time, the side-lobe intensity is suppressed well while the focal spot size is almost constant. This continuous phase filter can be produced by using diffraction optics[21] or spatial light modulators[22].

X. Ye's e-mail address is yexueh@126.com.

References

1. S. M. Mansfield and G. S. Kino, Appl. Phys. Lett. **57,** 2615 (1990).
2. B. D. Terris, H. J. Mamin, D. Rugar, W. R. Studenmund, and G. S. Kino, Appl. Phys. Lett. **65,** 388 (1994).
3. J. Wang and T. Hong, Chin. Opt. Lett. **2,** 722 (2004).
4. F. He, G. Cheng, X. Feng, D. Zhang, Z. Cheng, Q. Liu, W. Zhao, G. Chen, and X. Hou, Chin. Opt. Lett. **2,** 423 (2004).
5. L. P. Ghislain and V. B. Elings, Appl. Phys. Lett. **72,** 2779 (1998).
6. L. P. Ghislain, V. B. Elings, K. B. Crozier, S. R. Manalis, S. C. Minne, K. Wilder, G. S. Kino, and C. F. Quate, Appl. Phys. Lett. **74,** 501 (1999).
7. S. B. Ippolito, S. A. Thorne, M. G. Eraslan, B. B. Goldberg, and M. S. Ünlü, Appl. Phys. Lett. **84,** 4529 (2004).
8. M. Yoshita, K. Koyama, M. Baba, and H. Akiyama, J. Appl. Phys **92,** 862 (2002).
9. J. Zhang, C. W. See, M. G. Somekh, M. C. Pitter, and S. G. Liu, Appl. Phys. Lett. **85,** 5451 (2004).
10. V. Zwiller and G. Björk, J. Appl. Phys. **92,** 660 (2002).
11. Y. Lu, J. Xie, J. Zhang, H. Ming, and P. Wang, Opt. Commun. **203,** 87 (2002).
12. Y. Zhang, C. Zheng, and Y. Zou, Optik **115,** 277 (2004).
13. Y. Lu, J. Xie, and H. Ming, Opt. Commun. **215,** 251 (2003).
14. Y. Zhang, H. Xiao, and C. Zheng, New Journal of Physics **6,** 75 (2004).
15. Y. Zhang, J. Mod. Opt. **53,** 1919 (2006).
16. Y. Zhang and X. Ye, Appl. Phys. B **86,** 97 (2007).
17. Y. Zhang, Appl. Opt. **45,** 4540 (2006).
18. L. E. Helseth, Opt. Commun. **191,** 161 (2001).
19. P. Török and P. Varga, Appl. Opt. **36,** 2305 (1997).
20. S. B. Ippolito, B. B. Goldberg, and M. S. Ünlü, J. Appl. Phys. **97,** 053105 (2005).
21. D. M. de Juana, J. E. Oti, V. F. Canales, and M. P. Cagigal, Opt. Lett. **28,** 607 (2003).
22. J. Kang, W. Zhang, H. Wei, S. Chen, and J. Zhu, Chin. Opt. Lett. **4,** 184 (2006).